Regular Article

blood

LYMPHOID NEOPLASIA

Pathogenic role of B-cell receptor signaling and canonical NF-κB activation in mantle cell lymphoma

Nakhle S. Saba,[1,2] Delong Liu,[1] Sarah E. M. Herman,[1] Chingiz Underbayev,[1] Xin Tian,[3] David Behrend,[1] Marc A. Weniger,[1] Martin Skarzynski,[1] Jennifer Gyamfi,[1] Lorena Fontan,[4] Ari Melnick,[4] Cliona Grant,[5] Mark Roschewski,[5] Alba Navarro,[6] Sílvia Beà,[6] Stefania Pittaluga,[7] Kieron Dunleavy,[5] Wyndham H. Wilson,[5] and Adrian Wiestner[1]

[1]Hematology Branch, National Heart, Lung, and Blood Institute, National Institutes of Health, Bethesda, MD; [2]Section of Hematology and Medical Oncology, Department of Medicine, Tulane University, New Orleans, LA; [3]Office of Biostatistics Research, National Heart, Lung, and Blood Institute, National Institutes of Health, Bethesda, MD; [4]Division of Hematology and Medical Oncology, Department of Medicine, Weill Cornell Medical College, New York, NY; [5]Lymphoid Malignancies Branch, Center for Cancer Research, National Cancer Institute, National Institutes of Health, Bethesda, MD; [6]Institut d'Investigacions Biomediques August Pi i Sunyer, Barcelona, Spain; and [7]Laboratory of Pathology, National Cancer Institute, National Institutes of Health, Bethesda, MD

Key Points

- Activation of BCR and canonical NF-κB signaling in the lymph node correlates with survival in MCL.
- Mutations and polymorphisms in BCR and NF-κB pathways may confer cell autonomous signaling and affect response to ibrutinib.

To interrogate signaling pathways activated in mantle cell lymphoma (MCL) in vivo, we contrasted gene expression profiles of 55 tumor samples isolated from blood and lymph nodes from 43 previously untreated patients with active disease. In addition to lymph nodes, MCL often involves blood, bone marrow, and spleen and is incurable for most patients. Recently, the Bruton tyrosine kinase (BTK) inhibitor ibrutinib demonstrated important clinical activity in MCL. However, the role of specific signaling pathways in the lymphomagenesis of MCL and the biologic basis for ibrutinib sensitivity of these tumors are unknown. Here, we demonstrate activation of B-cell receptor (BCR) and canonical NF-κB signaling specifically in MCL cells in the lymph node. Quantification of BCR signaling strength, reflected in the expression of BCR regulated genes, identified a subset of patients with inferior survival after cytotoxic therapy. Tumor proliferation was highest in the lymph node and correlated with the degree of BCR activation. A subset of leukemic tumors showed active BCR and NF-κB signaling apparently independent of microenvironmental support. In one of these samples, we identified a novel somatic mutation in *RELA* (E39Q). This sample was resistant to ibrutinib-mediated inhibition of NF-κB and apoptosis. In addition, we identified germ line variants in genes encoding regulators of the BCR and NF-κB pathway previously implicated in lymphomagenesis. In conclusion, BCR signaling, activated in the lymph node microenvironment in vivo, appears to promote tumor proliferation and survival and may explain the sensitivity of this lymphoma to BTK inhibitors. (*Blood*. 2016;128(1):82-92)

Introduction

Mantle cell lymphoma (MCL) is an aggressive, largely incurable, subtype of non-Hodgkin lymphoma (NHL).[1,2] The genetic hallmark of MCL is the chromosomal translocation t(11;14)(q13;q32), which results in Cyclin-D1 overexpression. The translocation occurs during the pre-B stage of differentiation, and the malignant transformation has been thought to arise within naïve B cells.[3] In agreement, in most cases, the tumor cells express an unmutated (germ line configuration) immunoglobulin heavy chain (*IGHV*) gene. However, recognition of a restricted *IGHV* repertoire used by some tumors and identification of a less aggressive MCL variant expressing mutated *IGHV* genes suggest a possible role of antigenic selection in these tumors.[4,5]

Cyclin-D1 expression alone is not sufficient for malignant transformation, and additional events are required for oncogenesis.[3,6] Genomewide studies using next-generation sequencing identified several recurrently mutated genes including *ATM* and *TP53* (DNA damage response); *CCND1* and *RB1* (cell cycle); *MLL2*, *MLL3*, and *SMARCA4* (epigenetic modifiers); *UBR5* (*N*-end rule pathway); *NOTCH1/2* (Notch signaling pathway); and *BIRC3* and TRAF2 (NF-κB pathway).[7-9] Notably, most tumors do not contain mutations in signaling pathways amenable to therapeutic targeting.[10]

Although a few patients present with indolent disease and can be managed with an observant approach,[11,12] most have a rapidly progressive disease course requiring urgent intervention.[1,2] Despite long-lasting responses achieved with aggressive therapy, late relapses occur.[13] Thus, new therapeutic approaches for MCL are urgently needed.[1,2] Bortezomib, lenalidomide, and ibrutinib are drugs that the US Food and Drug Administration recently approved for treating MCL.[1,2] However, the mechanisms underlying MCL's sensitivity to these agents are not well understood.[10,14] Bortezomib, a proteasome inhibitor, can interfere with NF-κB activation. Although activating mutations in components of the NF-κB pathway have been described in MCL, they preferentially affect the alternative NF-κB

Submitted November 13, 2015; accepted April 23, 2016. Prepublished online as *Blood* First Edition paper, April 28, 2016; DOI 10.1182/blood-2015-11-681460.

The data reported in this article have been deposited in the Gene Expression Omnibus database (accession numbers GSE70910 and GSE70926).

The online version of this article contains a data supplement.

The publication costs of this article were defrayed in part by page charge payment. Therefore, and solely to indicate this fact, this article is hereby marked "advertisement" in accordance with 18 USC section 1734.

Downloaded from http://ashpublications.net/blood/article-pdf/128/1/82/1395848/82.pdf by guest on 02 June 2024

pathway and are found in only a small subset of tumors.[8,15] Furthermore, bortezomib induces cell death in MCL through oxidative and endoplasmic reticulum stress, resulting in the upregulation of the proapoptotic protein NOXA, a response independent of NF-κB inhibition.[16,17] Lenalidomide is an immunomodulatory agent with pleotropic effects that may include immune modulation and disruption of tumor-microenvironment interactions.[18,19]

Ibrutinib covalently binds Bruton tyrosine kinase (BTK), thereby irreversibly inactivating the kinase.[20] BTK is essential for B-cell receptor (BCR) signaling, and loss-of-function mutations lead to the virtual absence of mature B cells. A phase I trial of ibrutinib in patients with relapsed NHL demonstrated a high response rate in MCL, an unexpected finding that was confirmed in a disease-specific phase II trial demonstrating objective responses in 68% of patients, including 21% with complete response, and an overall survival (OS) rate of 58% at 18 months.[21,22]

Unlike MCL, ibrutinib's activity in chronic lymphocytic leukemia (CLL) and activated B-cell-like diffuse large B-cell lymphoma (ABC-DLBCL) is consistent with the documented role of BCR signaling in these diseases. In CLL, BCR signaling in the tumor cells is induced within the lymph node (LN) microenvironment.[23,24] However, the influence of the microenvironment on the pathogenesis of MCL has not been thoroughly investigated.[3] In ABC-DLBCL, chronic active BCR signaling has been linked to somatic mutations in *CD79B*.[25] Moreover, the high efficacy of ibrutinib in Waldenström macroglobulinemia is attributed to activation of BTK through mutant *MYD88*.[26,27] MCL rarely has mutations in *CD79B* and *MYD88*,[9,28] whereas the reported mutations in *TRAF2* and *BIRC3* activate the alternative NF-κB pathway, resulting in resistance, rather than sensitivity, to ibrutinib.[8] Thus, identification of pathogenic signaling pathways in MCL and the biologic basis for ibrutinib sensitivity require further investigation.

To investigate tumor-microenvironment interactions in vivo and gain further insights into MCL biology, we took advantage of the presence of tumor cells in different anatomic compartments. Specifically, we compared gene expression profiles and the activity of signaling pathways in tumor samples collected from the peripheral blood (PB) and LNs. We found evidence for active BCR and NF-κB signaling that, in most cases, is induced specifically in LN-resident MCL cells and determines OS.

Methods

Study design and patient samples

This translational laboratory study was performed with human LN and PB samples obtained from 43 patients with previously untreated MCL (supplemental Table 1, available on the *Blood* Web site). Patients were enrolled in a National Cancer Institute Institutional Review Board–approved study (registered with www.clinicaltrials.gov as NCT00114738) and treated with 6 cycles of bortezomib in combination with EPOCH-R (etoposide, prednisone, vincristine, doxorubicin, and rituximab). All samples were obtained with written informed consent. The laboratory study includes all patients with available gene expression data. Confirmatory studies by flow cytometry and in vitro testing were done for patients with sufficient leftover material.

Mononuclear cells from blood and LN single-cell suspension were isolated using density gradient centrifugation with lymphocyte separation medium (ICN Biomedicals). Fresh cells were subjected to CD19 selection using magnetic beads yielding purity >96% (Miltenyi Biotec). Normal (non-MCL) B cells were not detectable in PB samples of 15 of 17 patients analyzed. In 2 patients, normal B cells made up 0.2% and 0.3% of all B cells in the sample. Fixed LN biopsies were stained for Ki67 (DakoCytomation) after deparaffinization and quantified using Aperio Digital Pathology (Leica Microsystems). As previously described, *IGHV* sequencing was performed on leukemic samples and classified as mutated (<97% homology to germ line) or unmutated (≥97% homology).[4]

Flow cytometry

Antibodies for cell surface stain were (phycoerythrin [PE]-Cy5 anti-CD19, PE-Cy7 anti-CD5, PE anti-CD69, and PE anti-CD80). After surface staining, cells were washed and suspended in 4% paraformaldehyde (on ice, 1 hour), washed, resuspended in 70% ethanol (at −20°C, 2 hours), washed, incubated with intracellular stain (fluorescein isothiocyanate–anti-Ki67; Alexa Fluor-488–anti-*p*-SYK, *p*-PLCγ, *p*-AKT, *p*-ERK, and *p*-p65) for 20 minutes at room temperature, washed, and analyzed on a BD FACSCanto II flow cytometer (BD Biosciences), as described.[24] All antibodies were purchased from BD Biosciences, except for Alexa Fluor-488 anti-*p*-AKT (Life Technologies). Data were analyzed using FlowJo software (Tree Star Inc).

In vitro treatment with ibrutinib, MI-2, and PS1145

Viably frozen PB mononuclear cells and LN single-cell suspensions were exposed to ibrutinib, MI-2, or PS1145 for 48 hours. Triplicates of 500 000 cells per 100 μL were plated in a 96-well plate. We used the CellTiter 96 AQ_{ueous} Assay dye reduction assay (Promega) to quantify cell viability. Ibrutinib and PS1145, respectively, were purchased from Selleckchem and Sigma-Aldrich, while the MALT1 inhibitor MI-2 was kindly provided by Ari Melnick (Weill Cornell Medical College, New York, New York).

Gene expression profiling

Microarray hybridization was conducted as previously described.[24] Briefly, total RNA was extracted using the RNeasy kit (QIAGEN) and profiled on Human Genome U133 Plus 2.0 arrays according to the manufacturer's instructions (Affymetrix). CEL files were imported into the Affymetrix Expression Console and normalized with the Robust Multiarray Average method. Primary gene expression data of the MCL samples are deposited in Gene Expression Omnibus (GEO) under accession number GSE70910. Consistent with the disease biology, *CCND1* mRNA was highly and consistently overexpressed in all the MCL samples compared with CLL samples shown for reference (data available at GEO under accession number GSE21029)[24] (supplemental Figure 1).

To derive the NIK gene signature, we extracted the signal intensities of the probe sets from the CEL files of the dataset of GEO accession ID: GSE52435[8] and normalized them using the Robust Multiarray Average method. Three separate comparisons of the NIK knockdown experiment were analyzed as follows: (1) NIKsh# 100 ng/mL DOX (n = 4) vs NIKsh# 0 ng/mL (n = 4); (2) NIKsh# 100 ng/mL vs NIKsh# 0 ng/mL DOX (n = 4) and NTC (n = 4); and (3) NIKsh# 100 ng/mL DOX (n = 4) vs NTC (n = 4). Using these comparisons, we identified (1) 102 probe sets/77 genes (1.5 fold change [FC], $P < .01$); (2) 226 probe sets/153 genes (1.5 FC, false discovery rate [FDR] < 0.2); and (3) 105 probe sets/83 genes (1.5 FC, $P < .01$) with detectable signal intensities in at least half of the arrays, respectively. Forty-five genes were common to all 3 analyses, 28 of which were expressed in both Z-138 and Maver-1 at baseline. These 28 genes were considered the NIK signature genes.

The BCR score in the validation set was computed using gene expression data of MCL LN biopsies reported by Rosenwald et al[29] available at http://llmpp.nih.gov/MCL/.

RNA sequencing

Polyadenylated RNA was enriched by 2 rounds of oligo(dT) selection (Invitrogen), followed by PA-seq library construction[30] and sequencing on Illumina HiSeq-2000 with paired 50-bp reads. We used MapSplice 2[31] to map RNA-seq reads to human genome hg19, Samtools package (DHI Group) to remove duplicate reads and create mpileup files, and VarScan package (Genome Institute, Washington University) for INDEL and single-nucleotide variant callings. RNA sequencing data are deposited in GEO under accession number GSE70926. Single-nucleotide variants and INDELs were annotated with Ensembl GRCh37. RNA sequencing data were used only to look for mutations/polymorphisms in candidate genes and were not used toward gene expression, which was based entirely on the Affymetrix microarray data described above.

Downloaded from http://ashpublications.net/blood/article-pdf/128/1/82/1395848/82.pdf by guest on 02 June 2024

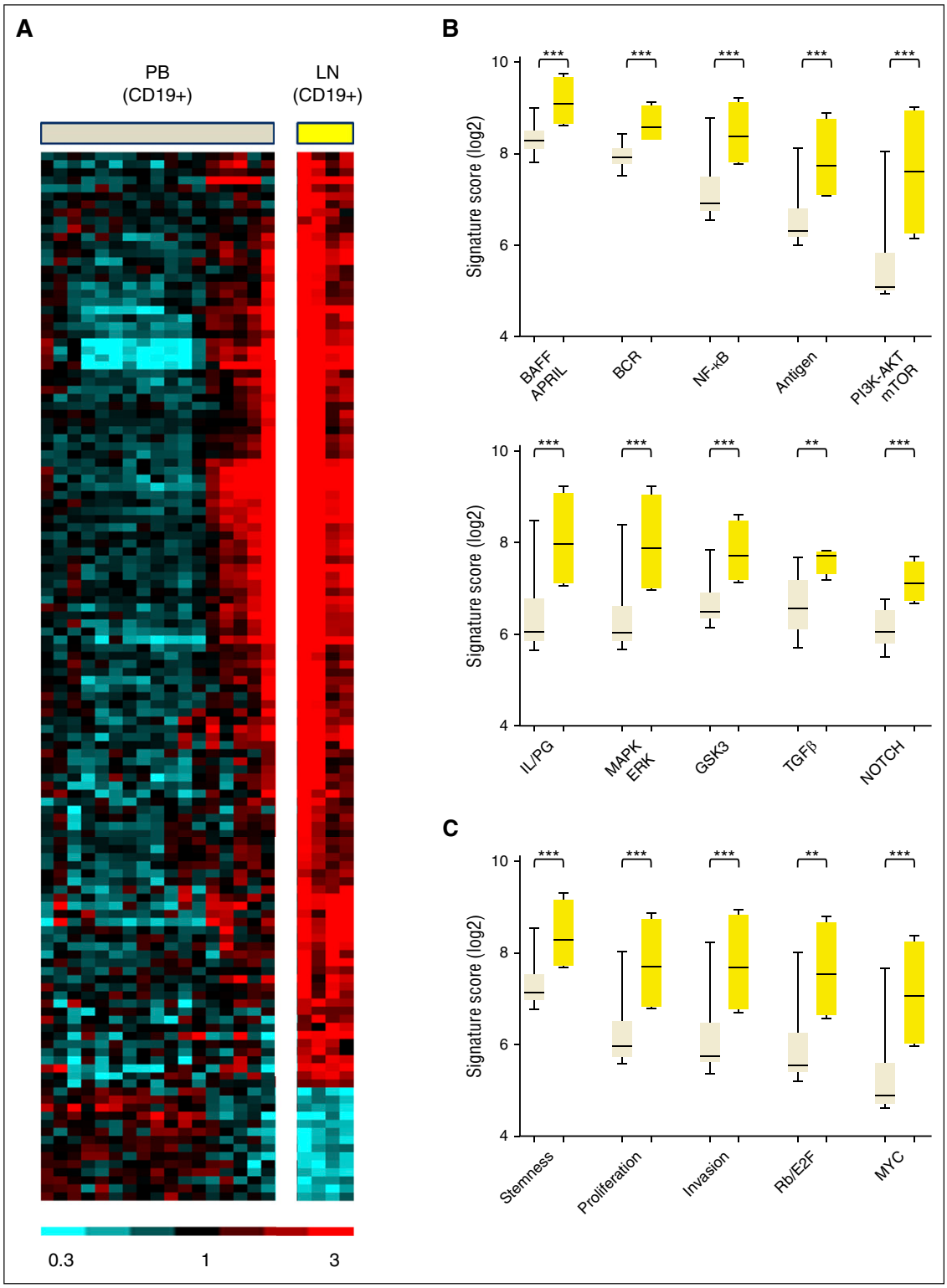

Figure 1. Gene expression differs between MCL cells in PB and LN due to activation of signaling pathways in the LN. (A) Heat map of 130 genes that were differentially expressed in purified MCL cells obtained from PB (PBT, n = 17) and LN (LNT, n = 4) in 18 patients (>2-fold change, FDR < 0.2). Gene expression data were median-centered. Relative expression is indicated by the color scale. (B and C) GSEA identified a large number of upregulated gene sets in LNT compared with PBT. Accordingly, 166 relevant gene sets were selected having FDR ≤ 0.01, NES ≥1.80, and ≥10 "leading edge genes" (the genes of a given gene set most significantly differentially expressed in the experimental data), then grouped into 4 categories based on their functional similarities (supplemental Table 3). Two of these 4 categories are displayed: (B) "Signaling and interaction with the microenvironment" and (C) "Proliferation/malignancy". Within each subcategory, the "signature score" of the gene set with the highest NES was calculated and displayed. This signature score was computed as the average of the mRNA expression level of the leading edge genes of a given gene set. The signature scores were compared between PBT and LNT samples using unpaired Student *t* test. AKT, protein kinase B; APRIL, a proliferation inducing ligand; BAFF, B-cell activating factor; E2F, E2F transcription factor; ERK, extracellular signal regulated kinase; GSK3, glycogen synthase kinase 3; IL, interleukin; LNT, purified tumor cells from LN; MAPK, mitogen-activated protein kinase; mTOR, mammalian target of rapamycin; MYC, v-myc avian myelocytomatosis viral oncogene homolog; PBT, purified tumor cells from PB; PG, prostaglandin; PI3K, phosphatidylinositol 3-kinase; Rb, retinoblastoma; TGFβ, transforming growth factor-β. ***$P < .001$; **$P < .01$.

Downloaded from http://ashpublications.net/blood/article-pdf/128/1/82/1395848/82.pdf by guest on 02 June 2024

Statistical analysis

The Student *t* test (paired or unpaired), Fisher's exact test, and one-way analysis of variance were used to assess the differences between groups. The probabilities of progression-free survival (PFS) and OS were calculated using the Kaplan-Meier method.[32] BCR scores were dichotomized using the optimal cutoff values for predicting progression and overall mortality.[33] All *P* values were 2-sided and *P* values $\leq .05$ were considered statistically significant. Analyses were performed using GraphPad Prism (GraphPad Software Inc), JMP software (SAS Institute), and R statistical software 3.2.2 (Institute for Statistics and Mathematics).

Results

Upregulation of survival and proliferation pathways in MCL cells in vivo is dependent on the LN microenvironment

We analyzed tumor samples from 43 previously untreated patients with MCL that were about to initiate therapy (supplemental Table 1). Consistent with the typical clinical presentation, the majority of patients had LN involvement, 40% had leukemic disease, and over 20% had both nodal and leukemic disease. In 34 patients, LN biopsies were obtained: in 30 by core biopsy and in 4 by surgical excision. In 8 patients, tumor cells were obtained concurrently from both blood and LN. Nine patients provided only blood samples. In summary, 55 samples were analyzed: 17 leukemic samples, 34 LN biopsies, and 4 LN single-cell suspensions.

To identify intracellular signaling pathways activated in MCL cells within the lymphoid tissues, we compared gene expression in MCL cells purified by CD19 selection from blood and LN (Figure 1A). By analysis of variance, 130 genes showed at least a 2-fold change in expression with FDR < 0.2. Of these differentially expressed genes, 116 were overexpressed in the LN-derived tumor cells, whereas only 14 were overexpressed in the PB-derived tumor cells (supplemental Table 2). To identify the biologic basis for the differences in gene expression, we chose Gene Set Enrichment Analysis (GSEA) as employed previously.[24] GSEA identified 458 curated gene sets that were enriched in tumor cells in the LN compared with their circulating counterparts in the blood at FDR ≤ 0.01 and normalized enrichment score (NES) ≥ 1.80. Of these, 166 gene sets relevant to lymphoma reflect activation of signaling pathways and tumor proliferation in the LN. Based on their functional similarities, the gene sets were grouped into 4 distinct categories (Figure 1B-C; supplemental Table 3): "Signaling and Interaction with the Microenvironment" comprising 27 gene sets, including BCR, NF-κB, and PI3K-AKT-mTOR (Figure 1B); "Proliferation and Malignancy" comprising 103 gene sets (Figure 1C); "DNA Damage Pathways" (19 gene sets); and "Other" (17 gene sets).

Activation of the BCR and canonical NF-κB pathways in MCL cells

Using experimentally validated BCR and NF-κB gene signatures,[24] we investigated the activation of these pathways in a large cohort of patients having contributed LN core biopsies. The BCR gene signature consisting of 27 genes was highly expressed in LN but less so in most leukemic samples (Figure 2A). As a quantitative measure of BCR signaling, we used a gene signature score computed as the averaged expression of all genes in the BCR signature. Across all samples, the median BCR signature score increased in the nodal as compared with the leukemic tumors ($P < .0001$; Figure 2B, left panel). Ruling out that the observed differences were due to interpatient variability, we specifically confirmed upregulation of BCR signaling in the LN in matched pairs of nodal and leukemic samples obtained concurrently from the same patient ($n = 8$; Figure 2B, middle panel). Interestingly, in 7 of 17 patients with leukemic MCL, the BCR scores in PB-derived tumor cells were comparable to that in the nodal samples.

Three NF-κB gene sets were identified as upregulated in nodal compared with leukemic tumors by GSEA. Next, we used 2 experimentally validated gene signatures to separately probe the activity of the canonical and alternative NF-κB pathways (Figure 2C-F). The canonical NF-κB signature, consisting of 18 genes dependent on IKKβ activation,[24,34] was on average 2.1-fold more highly expressed in LN biopsies compared with purified MCL cells ($P < .0001$). Consistent with BCR-dependent activation of NF-κB signaling, the 2 signature scores were highly correlated ($r = 0.88$; $P < .0001$; data not shown).

Akin to the distribution of the BCR score, the NF-κB score clearly dichotomized leukemic samples into 2 subsets: a subset with NF-κB scores in the blood consistently lower than in nodal samples and a second subset with NF-κB scores that were equally high in leukemic and nodal samples (Figure 2D, left panel). Thus, the first set of tumors appears to depend on the LN environment for activation of BCR and NF-κB pathways, whereas in the second set, signaling could be either independent of the LN microenvironment or more sustained once cells exit the tissue.

To probe activation of the alternative NF-κB pathway, we used a gene signature dependent on NIK expression[8] (see "Methods" for details). The NIK signature was also more highly expressed in LN biopsies compared with purified MCL cells (average fold change 1.6; $P < .0001$; Figure 2E-F). Overall, NIK signature genes were less well expressed and showed less variability in expression between patients and anatomic compartments than the canonical NF-κB signature genes. Furthermore, although the BCR and NF-κB signatures were equally expressed in excisional nodal biopsies and tumor cells purified from these biopsies (Figure 2B,D, right panels), the NIK signature was more highly expressed in the LN biopsies compared with matching purified tumor cells (average fold change 1.4; $P < .05$; Figure 2F, right panel), suggesting that genes regulated through the alternative NF-κB pathway are preferentially expressed by nontumor cells in the LN microenvironment.

Activation and propagation of BCR and NF-κB signaling and tumor proliferation

Antigen-dependent BCR signaling is propagated through phosphorylation of kinases that activate different downstream pathways.[20] To query sequential activation steps in the BCR signaling pathway, we used flow cytometry to detect phosphorylation of SYK, PLCγ, ERK, AKT, and the NF-κB transcription factor p65. Two representative patients with available leukemic blood samples and matched LN single-cell suspensions (MCL-21 and MCL-28) were analyzed in detail (Figure 3A-C). In both patients, BCR and NF-κB signature scores in the LN were approximately double the respective scores in the blood (Figure 3A). The LN resident cells also contained more activated signaling proteins at every node of the pathway compared with matched leukemic cells (Figure 3B-C). Levels of $p\text{-SYK}^{Y348}$ and the BCR signature score were highly correlated in all 14 patients with available samples (Figure 3D).

Among the 166 gene sets upregulated in the LN, 52 gene sets were related to tumor proliferation. In addition, a previously reported MCL-derived proliferation signature[29] was more highly expressed in nodal compared with leukemic tumors, both among all samples (average fold change 2.5, $P < .0001$) and among patient-matched samples ($n = 8$; average fold change 3.2; $P < .0001$) (Figure 4A). Next, we assessed

Downloaded from http://ashpublications.net/blood/article-pdf/128/1/82/1395848/82.pdf by guest on 02 June 2024

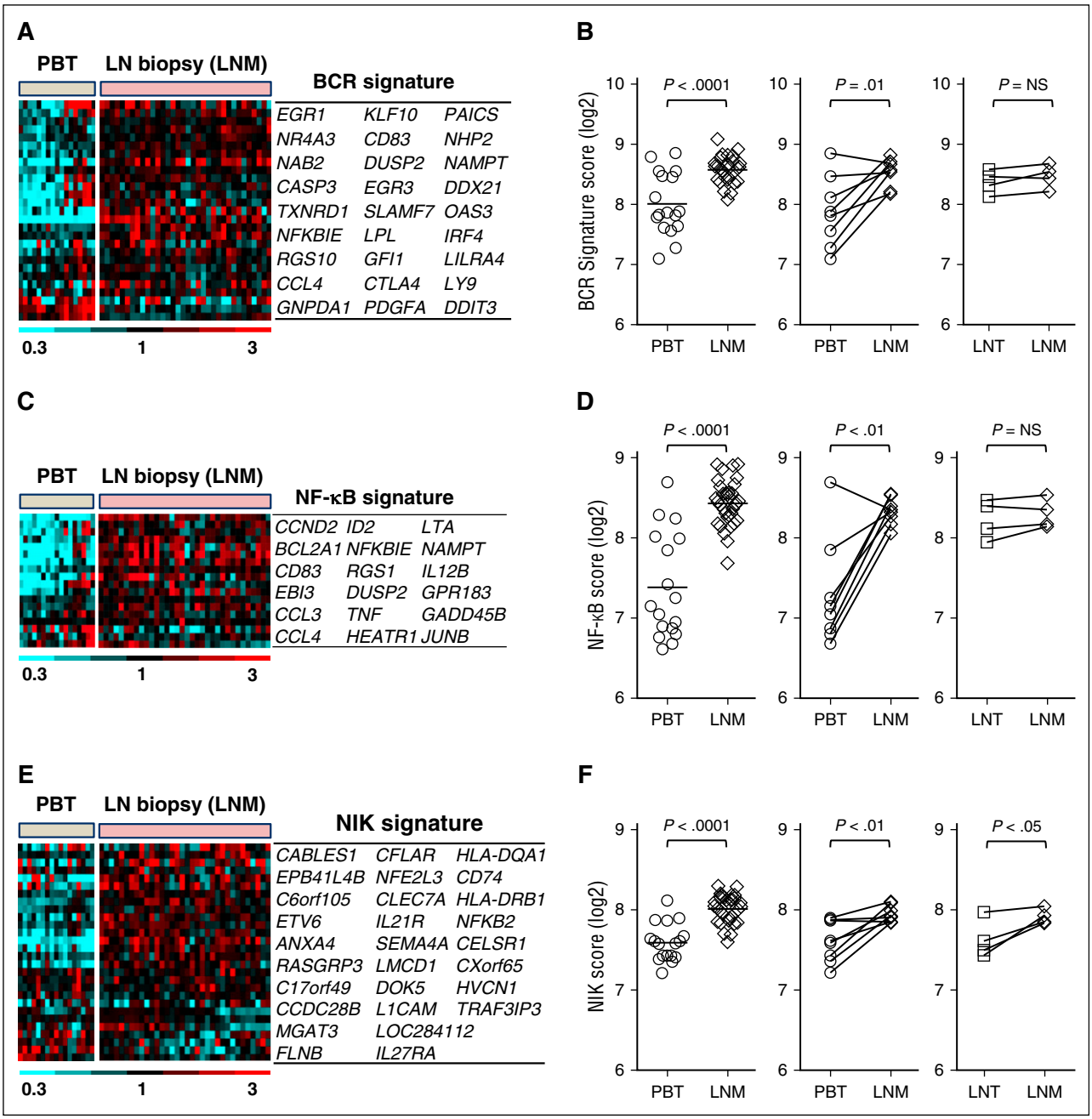

Figure 2. Activation of BCR and NF-κB signaling and tumor proliferation in LN-resident cells. (A) Twenty-seven genes comprising a previously validated BCR gene signature are depicted in a heat map. Gene expression data were median-centered and scaled as indicated. Each column represents a patient's sample; each row represents a gene. Genes are vertically arranged in the corresponding table, following the same order as in the heat map. (B) The BCR signature score was computed by averaging the mRNA expression level of all signature genes. Signature scores between PBT and LNM groups were compared using unpaired Student *t* test (left panel). BCR scores in matched MCL PBT/LNM (n = 8) and LNT/LNM (n = 4) samples were compared using paired Student *t* test (right panels). Matched samples were concomitantly collected from the same patient and are connected with a line. (C) Heat map of 18 genes representing the canonical NF-κB pathway (NF-κB signature) generated after a supervised clustering of the samples. Patients' samples and gene names are arranged in columns and rows, respectively. Genes are vertically arranged in the corresponding table, following the same order as in the heat map. (D) The NF-κB signature scores of MCL PBT, LNM, and LNT were compared as in (B). (E) Heat map of 28 genes representing the alternative NF-κB pathway (NIK signature) generated after a supervised clustering of the samples. Patients' samples and gene names are arranged in columns and rows, respectively. Genes are vertically arranged in the corresponding table, following the same order as in the heat map. (F) The NIK signature scores of MCL PBT, LNM, and LNT were compared as in (B). LNM, whole lymph node biopsy.

tumor proliferation by Ki67 expression using immunohistochemistry in LN biopsies and flow cytometry of $CD5^+/CD19^+$ gated tumor cells. The proliferation signature score and the number of Ki67-positive tumor cells was highly correlated in both leukemic ($r = 0.93$; $P < .0001$) and nodal tumors ($r = 0.79$; $P < .0001$) (data not shown). Furthermore, in patients with matched blood and LN samples, Ki67 expression was clearly increased in the nodal compared with the leukemic tumor population (Figure 4B-C). Similarly, expression of activation markers CD69 and CD80 was significantly higher in the nodal tumors (Figure 4D).

The BCR score significantly correlated with the proliferation score of nodal samples (Figure 4E; $r = 0.47$; $P = .006$), and the percent

Downloaded from http://ashpublications.net/blood/article-pdf/128/1/82/1395848/82.pdf by guest on 02 June 2024

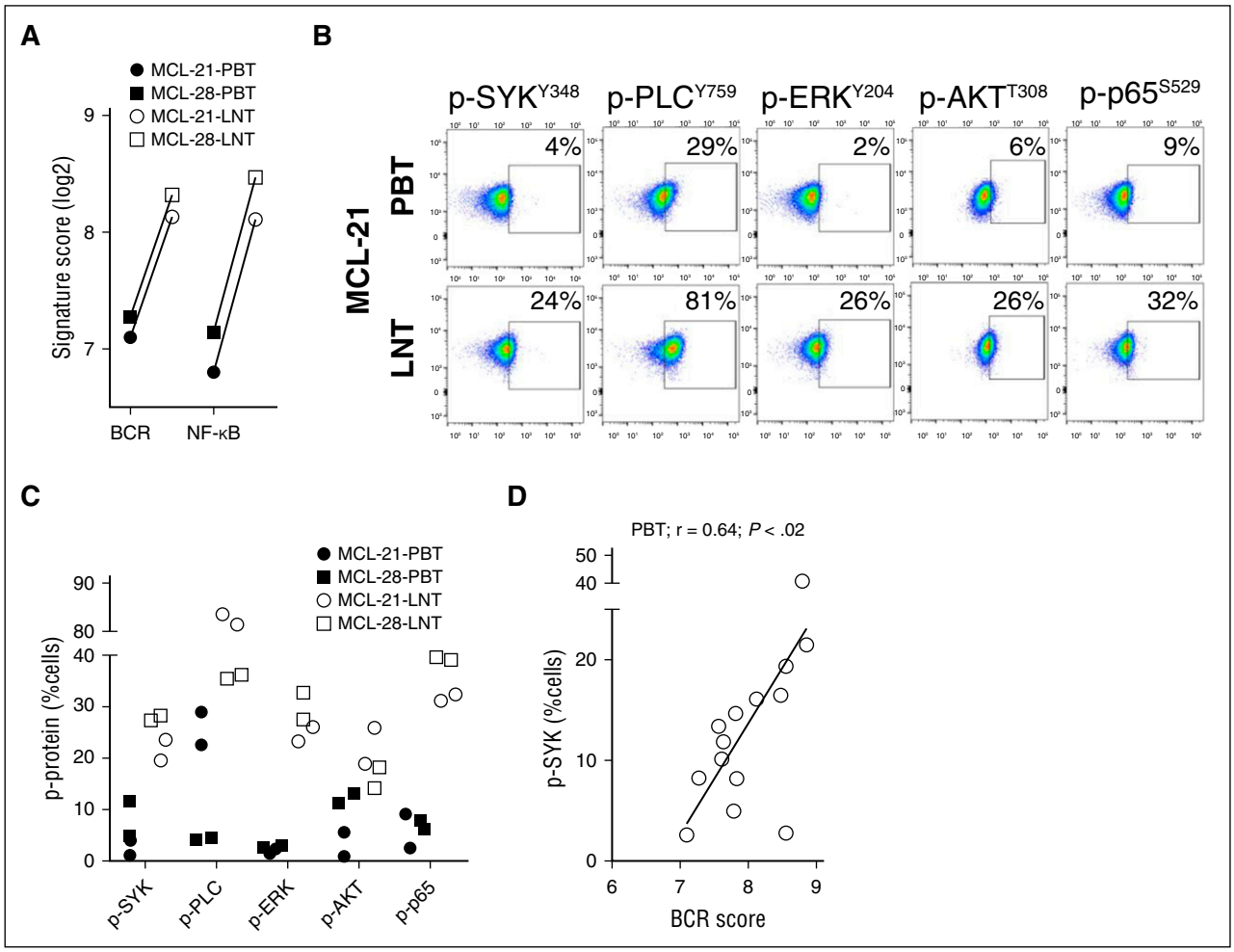

Figure 3. Activation of signal transduction components of the BCR and downstream pathways. Phosphorylation of SYK, PLCγ, ERK, AKT, and p65 was assessed by flow cytometry in $CD5^+/CD19^+$ MCL cells from the PB and LN. (A) Comparison of the BCR and NF-κB signature scores between PBT and LNT samples concomitantly isolated from 2 patients providing matched cell samples. (B) Flow plots of PB and LN samples from a representative patient are shown. (C) Summary of phosphoprotein analysis (tested in duplicate) for matched PB and LN samples from the 2 patients shown in (A). (D) Pearson correlation *r* was used to measure the relationship of the percent tumor cells with detectable *p*-SYK and the corresponding BCR signature score in MCL-PBT (n = 14).

Ki67-positive cells in the LN (Figure 4F; $r = 0.39$; $P = .03$), indicating that tumors with strong BCR signaling are also more proliferative.

Activity of BCR predicts patient survival after cytotoxic therapy

To examine whether the strength of BCR signaling impacts the survival of patients with MCL, we divided patients into 2 groups based on the BCR score in the LN. Patients having a BCR score in the upper tercile had significantly lower PFS (hazard ratio [HR] 2.26; $P = .04$) and OS (HR = 6.88; $P = .05$) compared with all other patients (Figure 5A-B). With a median follow-up of 7.5 years, OS for patients with high BCR scores was 68% compared with 96% for patients with lower BCR scores. To validate our finding in an independent set of patients, we computed the BCR score in gene expression data of MCL LN biopsies reported by Rosenwald et al.[29] Using the same approach to dichotomize the patients in the validation set, a BCR score in the upper tercile identified patients with inferior survival (HR = 1.81; $P = .03$; Figure 5C). In the combined patients from both studies ($n = 126$), the median survival time was 3.1 years for patients with BCR score in the upper tercile compared with 5.5 years for all other patients (HR 1.69; $P = .04$; Figure 5D). Similarly, the 7 patients whose leukemic samples showed a BCR score above mean had inferior survival compared with the rest of the group, albeit without reaching statistical significance (supplemental Figure 2A-B).

Point mutations in signal transduction components of the BCR and NF-κB pathways and response to BTK inhibition

A subset of leukemic samples showed active BCR and NF-κB signaling apparently independent of microenvironmental support. Among 7 samples with BCR scores above mean, the *IGHV* gene was mutated in 1 (MCL-51), unmutated in 4, and undetermined in 2. All tested samples with BCR scores below mean were *IGHV* unmutated (supplemental Table S1). We next searched for mutations in genes encoding components of the BCR and NF-κB signaling pathways. Using RNA sequencing, we identified numerous nonsynonymous mutations in 137 genes that encode components of the BCR and NF-κB pathways (supplemental Table 4). Mutations listed in the SNP137 database were deemed polymorphisms and were not considered further. To explore the predicted consequence of mutations on protein structure and function, we used the PolyPhen-2, PROVEAN, Mutation Taster, and PhD-SNP software packages. Mutations that were predicted to have a significant effect on the protein's structure and/or function by at least 2 programs were considered further and referred to

Downloaded from http://ashpublications.net/blood/article-pdf/128/1/82/1395848/82.pdf by guest on 02 June 2024

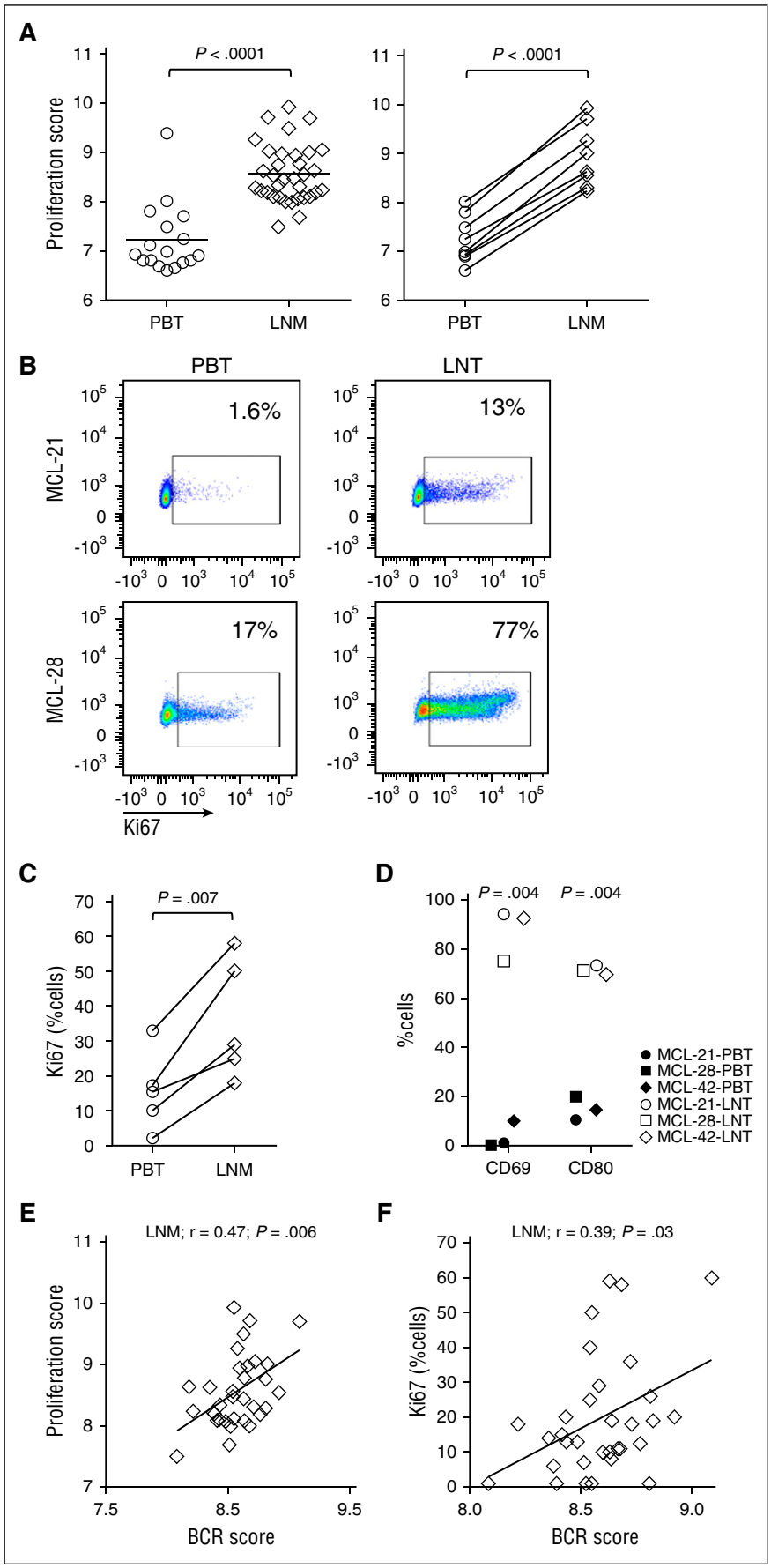

Figure 4. The LN microenvironment promotes tumor activation and proliferation. (A) The MCL-proliferation score was compared between PBT and LNM groups using unpaired Student *t* test (left panel). MCL-proliferation scores in matched MCL PBT/LNM (n = 8) samples were compared using paired Student *t* test (right panel). (B) Representative PBT and LNT samples from 2 patients with MCL were tested for Ki67 using flow cytometry. (C) Comparison of Ki67-positive cells between PBT and LNM (n = 5) samples concomitantly collected from the same patient. (D) The activation markers CD69 and CD80 were measured using flow cytometry in $CD5^+/CD19^+$-gated cells of matched PBT and LNT from 3 patients with MCL. Pearson correlations of the (E) proliferation score in LN biopsies (LNM, n = 34) and (F) the percent Ki67-positive cells in LNM (n = 32) quantified by immunohistochemistry, with the corresponding BCR signature score.

Downloaded from http://ashpublications.net/blood/article-pdf/128/1/82/1395848/82.pdf by guest on 02 June 2024

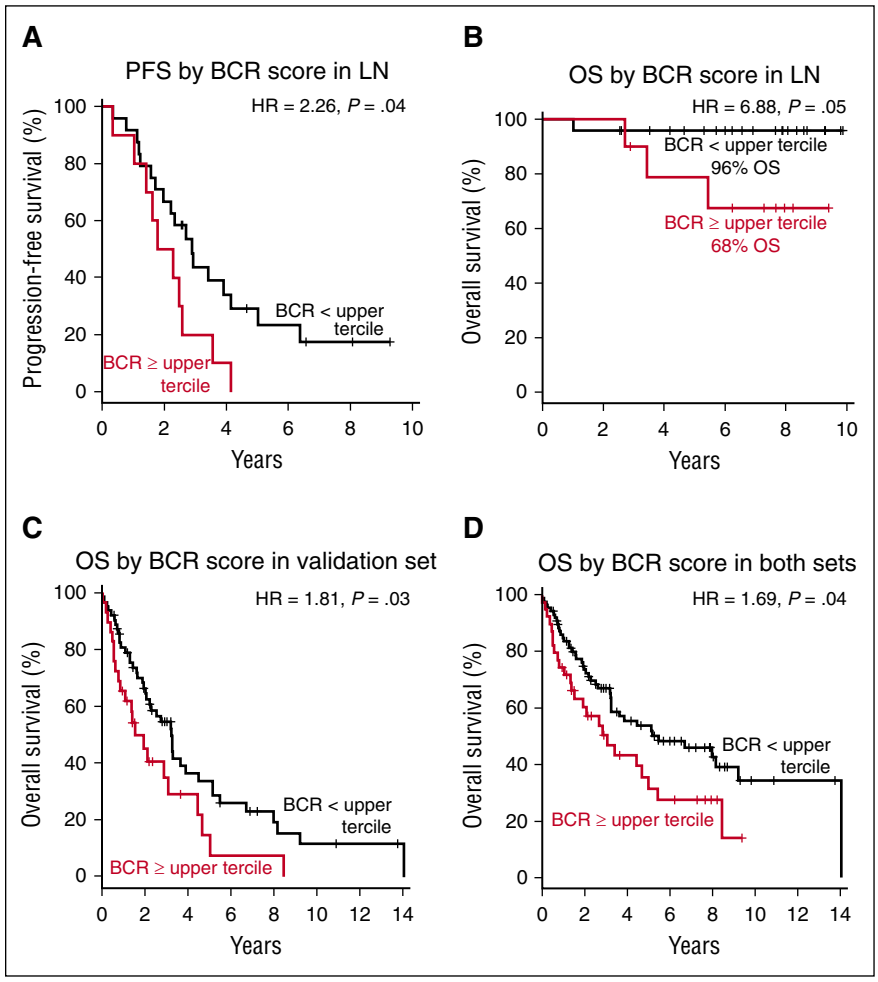

Figure 5. BCR score predicts for PFS and OS in MCL. Probabilities of PFS and OS were compared in subgroups dichotomized by BCR score measured in the LN samples using the log-rank test. The median OS or PFS time was calculated as the smallest survival time when the survival probability is ≤50%. (A) The median PFS time for patients with BCR score within the upper tercile was 2.0 years and was 2.9 years for the remaining patients. (B) At the median follow-up of 7.5 years, the estimated OS for patients with BCR score in the upper tercile was 68% and was 96% for the remaining patients. The median OS time for patients dichotomized by BCR score was (C) in an independent validation set 1.5 years and 3.2 years, respectively, and (D) in both sets combined (n = 126) 3.1 and 5.5 years, respectively.

as "relevant mutations" (supplemental Table 5). A total of 12 relevant mutations in 11 genes were identified (Figure 6A). Six of 7 leukemic samples (86%) with a high BCR score carried at least one mutation. By contrast, relevant mutations were identified in only 2 of 9 (22%) samples having a low BCR score ($P = .01$ by Fisher's exact test for the overrepresentation of relevant mutations in tumor samples with high BCR score). Only *IKBIP* V186G and *SHARPIN* R365H have been previously reported in COSMIC; however, neither has been confirmed as somatic.

To investigate which mutations are somatic, we performed Sanger sequencing on tumor and nontumor DNA. Of 8 relevant mutations (*RELA* E39Q, *TNFRSF13C* H159Y, *IKBIP V186G*, *PLCG2* M28L, *RNF31* R941Q, *BIRC6* N3110S, *ITPR2* T2184S, and *SHARPIN* R365H), only the E39Q mutation in *RELA* in MCL51 was confirmed as somatic (supplemental Figure 3A-H). Previously reported mutations in *TRAF2* and *BIRC3* were not observed.[8]

To explore whether mutations in signal transduction components could promote BCR-independent activation of NF-κB, we simultaneously assessed the phosphorylation state of SYK and p65 by flow cytometry (Figure 6B, supplemental Table 6). In nodal tumor cells, both SYK and p65 were highly phosphorylated, consistent with BCR-dependent activation of the canonical NF-κB pathway (Figure 6B). Also, in most leukemic samples, both SYK and p65 were concurrently activated. However, 1 leukemic sample (MCL-51) with 3 relevant mutations had low levels of *p*-SYK but high levels of *p*-p65, suggesting that NF-κB activation may occur independently of upstream BCR signaling (Figure 6B).

Next, we tested the effect of BTK inhibition by ibrutinib on p65 activation and viability of primary MCL cells in vitro. In samples having concordant levels of *p*-SYK and *p*-p65, ibrutinib reduced *p*-p65, consistent with BTK-dependent activation of NF-κB downstream of the BCR (Figure 6C) and killed 35% to 50% of the tumor cells within 48 hours (Figure 6D). In contrast, levels of *p*-p65 and viability of tumor cells from MCL-51 were not substantially affected by ibrutinib (Figure 6C-D). MCL-51 was also resistant to MALT1 and IKK inhibition by MI-2 and PS1145, respectively (Figure 6D).

Discussion

We provide direct in vivo evidence for BCR and canonical NF-κB activation in MCL cells within the LN microenvironment. The activity of BCR signaling directly correlated with increased tumor proliferation and identified a subset of patients with inferior survival, suggesting that activation of BCR signaling drives tumor proliferation and determines clinical outcomes of patients with MCL. Furthermore, we identified mutations in genes encoding components of the BCR and NF-κB pathways that may amplify the cellular response to BCR engagement

Downloaded from http://ashpublications.net/blood/article-pdf/128/1/82/1395848/82.pdf by guest on 02 June 2024

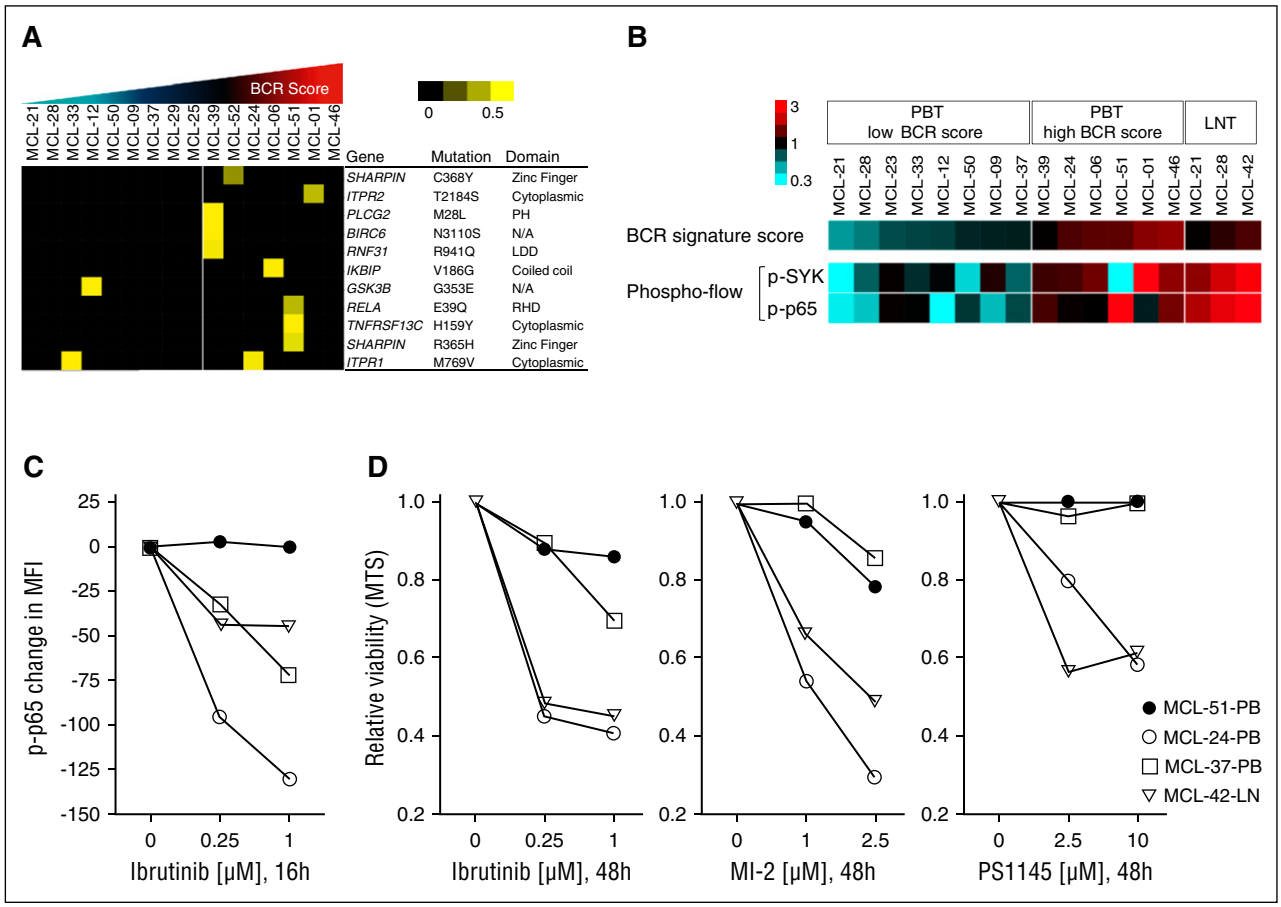

Figure 6. Mutations in signal transduction components, BCR signaling, and sensitivity to BTK inhibition. (A) Nonsynonymous mutations predicted to have a significant effect on the protein by at least 2 software programs were considered "relevant mutations." Sixteen leukemic MCL samples were subject to RNA sequencing. A set of 137 genes representing the BCR and NF-κB (canonical and alternative) pathways (supplemental Table 4) was tested for point mutations using the following filters: minimum number of reads: 8; minimum percent of mutated reads: 20; duplicate reads excluded; synonymous mutations and mutations listed in the SNP137 database excluded. Samples are displayed according to their ascending BCR signature score and divided in 2 groups: (1) BCR-low, n = 9; and (2) BCR-high, n = 7, based on the BCR score mean. Allele frequency is median-centered and scaled as indicated. Each column represents a patient sample and each row represents a gene. (B) The BCR signature score, and the levels of *p*-p65 and *p*-SYK (expressed as log2 of the percent positive cells among $CD5^+/CD19^+$-gated cells) were median-centered and displayed according to the color scale. Each column represents a patient's sample. Leukemic samples are arranged according to their BCR signature score. Suspension cells obtained from LN are shown on the far right for comparison (LNT). (C) Change in *p*-p65 MFI of 4 samples after exposure to ibrutinib, tested by flow cytometry. Each data point represents the mean of duplicates from 2 separate experiments. (D) MTS assay of samples as in (C) tested in triplicate against increasing concentrations of ibrutinib, the MALT1 inhibitor MI-2, and the IKK inhibitor PS1145 for 48 hours.

and promote BTK independent NF-κB activation and ibrutinib resistance.

Ongoing active BCR signaling contrasts with the tenet that MCL is a malignancy of antigen-naïve B cells and provides analogies to CLL and ABC-DLBCL where a role for BCR signaling in lymphomagenesis has been previously recognized.[24,25] In contrast to ABC-DLBCL, activating mutations in *CD79B* are rare in MCL.[9,28] Rather, in analogy to CLL, BCR activation in MCL cells appears dependent on tumor-microenvironment interactions in the LN. Although a role of antigen in the ontogeny of MCL has been inferred from the biased *IGHV* gene repertoire found in a subset of patients,[5] this is the first demonstration of ongoing active BCR signaling in tumor cells in vivo. A prior study using gene expression analysis of leukemic samples identified differences between *IGHV* unmutated and *IGHV* mutated samples, the latter showing higher expression of genes associated with memory B cells.[4] All leukemic cases studied here were of the *IGHV* unmutated type with the exception of MCL-51, the sample with the *RELA* mutation. The conclusion that BCR signaling plays a pathogenic role in MCL is consistent with emerging data on the role of *SOX11* in this lymphoma.[35-37] The transcription factor SOX11 enforces expression of the lineage master regulator PAX5.[1,37] PAX5 maintains the B-cell program and prevents terminal plasma-cell differentiation, thereby preserving the cellular responsiveness to antigen induced activation and proliferation.

For the subset of patients in whom expression of BCR and NF-κB target genes appeared to be less dependent on the tissue microenvironment, we considered that intracellular signaling could be due to mutations that activate the BCR in a cell-autonomous fashion or extend the duration of signaling once the cells exit the lymphoid microenvironment. Addressing this possibility, we used RNA sequencing and identified mutations in 11 of 137 genes that encode components of the BCR and NF-κB pathways. Mutations were present in all but 1 of the 7 leukemic samples with high BCR and NF-κB scores. Only the E39Q mutation in *RELA* was somatic, whereas the others were rare germ line variants. This is the first report of *RELA* E39Q mutation in cancer. The affected tumor (MCL-51) was unusual for having high levels of *p*-p65 but low levels of activated SYK and was resistant to inhibition of BTK, MALT1, and NF-κB in vitro. E39 is located in the DNA binding interface of p65 (RELA), and the mutation is predicted to result in a

Downloaded from http://ashpublications.net/blood/article-pdf/128/1/82/1395848/82.pdf by guest on 02 June 2024

functionally relevant change. Whether this mutation can result in stronger DNA binding or dimerization of the transcription factor remains to be determined. In addition, the *RELA* mutation in MCL-51 was accompanied by rare germ line variants in *TNFRSF13C* and *SHARPIN*, which could alter the cellular signaling capacity. The H159Y mutation in *TNFRSF13C*, the gene encoding B cell–activating factor receptor, has been associated with the risk of developing B-cell NHL.[38] Furthermore, mutations in *RNF31* and *SHARPIN*, both components of the linear ubiquitin chain assembly complex (LUBAC), were identified in 3 leukemic samples. LUBAC aggregates with CARD11-MALT1-BCL10 to activate NF-κB. Recurrent gain-of-function germ line variants in *RNF31* were reported in patients with ABC-DLBCL and shown to be required for ABC-DLBCL viability.[39] In contrast, we did not identify mutations reported by others in *TRAF2* and *BIRC3*[8] or any other component of the alternative NF-κB pathway, consistent with the low activity of NIK-dependent signaling in the patients studied here.

All patients who provided samples for this study were subsequently treated, mostly with bortezomib in combination with EPOCH-R. In contrast, the validation set consisted of a group of patients treated in the pre-rituximab era with a variety of different regimens.[29] This difference in treatment between the 2 cohorts likely explains why the OS of patients in the validation cohort was shorter than for patients in our study. Notwithstanding, in both cohorts highly active BCR signaling identified a subset of patients with inferior survival. Although we have not shown a direct link between BCR activation in the LN and disease progression, this can be reasonably inferred given the biologic role of BCR signaling in promoting expansion and maturation of antigen-responsive B cells. Furthermore, antigen-dependent BCR activation has been shown to accelerate disease progression in mouse lymphoma models and can drive early stages of mucosa-associated lymphoid tissue lymphomas.[40-42]

Our analysis of primary tumor samples revealed a previously unappreciated importance of BCR and canonical NF-κB signaling in the pathogenesis of MCL, underscoring the value of specifically targeting these pathways. However, depth and durability of response to BTK inhibition differ considerably between lymphoma subtypes.[21,22,43,44] The response rate of 68% to single-agent ibrutinib in relapsed/refractory MCL compares favorably with previously available treatment options for these patients. However, roughly one-third of patients have intrinsically resistant disease whose mechanisms are not well understood. The importance of the *RELA* E39Q mutation and the germ line polymorphisms in components of the BCR and canonical NF-κB pathways, identified here, await confirmation in patients treated with ibrutinib. To overcome ibrutinib resistance, targeting signal transduction downstream of BTK with inhibitors of LUBAC and/or the MALT1 protease should be explored.[39,45]

Acknowledgments

The authors thank their patients for participating and donating the blood and tissue samples to make this research possible. The authors thank Therese White and Margaret Shovlin for assistance in the clinic, Theresa Davis-Hill for preparing LN single-cell suspensions, Jun Zhu and the members of the DNA sequencing and genomics core for assistance with gene expression profiling and RNA sequencing, and Keyvan Keyvanfar for assistance with flow cytometry.

This work was funded by the Intramural Research Programs of the National Heart, Lung, and Blood Institute and the National Cancer Institute, National Institutes of Health.

Authorship

Contribution: N.S.S., S.E.M.H., C.U., and D.B. performed experiments. N.S.S. and A.W. designed the research, analyzed the results, made the figures, and wrote the manuscript. S.P. performed and analyzed the immunohistochemistry experiments. D.L. performed the biostatistical analysis and contributed to microarray and sequencing data analysis. A.M. and L.F. provided MI-2. S.B. and A.N. performed *IGHV* sequencing. N.S.S., A.W., M.A.W., M.S., J.G., C.G., M.R., K.D., and W.H.W. contributed to the study design and to manuscript writing. All authors read and approved the final manuscript.

Conflict-of-interest disclosure: A.W. received institutional research funding from Pharmacyclics. W.H.W. is an inventor on a patent application regarding the use of ibrutinib in ABC-DLBCL. N.S.S. has served on advisory boards and on the speaker's bureau for Pharmacyclics.

Correspondence: Adrian Wiestner, Hematology Branch, National Heart, Lung, and Blood Institute, National Institutes of Health, Bld 10, CRC 3-5140, 10 Center Dr, Bethesda, MD 20892-1202; e-mail: wiestnera@mail.nih.gov.

References

1. Campo E, Rule S. Mantle cell lymphoma: evolving management strategies. *Blood.* 2015;125(1):48-55.
2. Hoster E, Klapper W, Hermine O, et al. Confirmation of the mantle-cell lymphoma International Prognostic Index in randomized trials of the European Mantle-Cell Lymphoma Network. *J Clin Oncol.* 2014;32(13):1338-1346.
3. Jares P, Colomer D, Campo E. Molecular pathogenesis of mantle cell lymphoma. *J Clin Invest.* 2012;122(10):3416-3423.
4. Navarro A, Clot G, Royo C, et al. Molecular subsets of mantle cell lymphoma defined by the IGHV mutational status and SOX11 expression have distinct biologic and clinical features. *Cancer Res.* 2012;72(20):5307-5316.
5. Hadzidimitriou A, Agathangelidis A, Darzentas N, et al. Is there a role for antigen selection in mantle cell lymphoma? Immunogenetic support from a series of 807 cases. *Blood.* 2011;118(11):3088-3095.
6. Pérez-Galán P, Dreyling M, Wiestner A. Mantle cell lymphoma: biology, pathogenesis, and the molecular basis of treatment in the genomic era. *Blood.* 2011;117(1):26-38.
7. Meissner B, Kridel R, Lim RS, et al. The E3 ubiquitin ligase UBR5 is recurrently mutated in mantle cell lymphoma. *Blood.* 2013;121(16):3161-3164.
8. Rahal R, Frick M, Romero R, et al. Pharmacological and genomic profiling identifies NF-κB-targeted treatment strategies for mantle cell lymphoma. *Nat Med.* 2014;20(1):87-92.
9. Zhang J, Jima D, Moffitt AB, et al. The genomic landscape of mantle cell lymphoma is related to the epigenetically determined chromatin state of normal B cells. *Blood.* 2014;123(19):2988-2996.
10. Saba N, Wiestner A. Do mantle cell lymphomas have an 'Achilles heel'? *Curr Opin Hematol.* 2014;21(4):350-357.
11. Royo C, Navarro A, Clot G, et al. Non-nodal type of mantle cell lymphoma is a specific biological and clinical subgroup of the disease. *Leukemia.* 2012;26(8):1895-1898.
12. Martin P, Chadburn A, Christos P, et al. Outcome of deferred initial therapy in mantle-cell lymphoma. *J Clin Oncol.* 2009;27(8):1209-1213.
13. Geisler CH, Kolstad A, Laurell A, et al; Nordic Lymphoma Group. Nordic MCL2 trial update: six-year follow-up after intensive immunochemotherapy for untreated mantle cell lymphoma followed by BEAM or BEAC + autologous stem-cell support: still very long survival but late relapses do occur. *Br J Haematol.* 2012;158(3):355-362.

Downloaded from http://ashpublications.net/blood/article-pdf/128/1/82/1395848/82.pdf by guest on 02 June 2024

14. Colomer D, Campo E. Unlocking new therapeutic targets and resistance mechanisms in mantle cell lymphoma. *Cancer Cell.* 2014;25(1):7-9.
15. Camara-Clayette V, Lecluse Y, Schrader C, et al. The NF-κB pathway is rarely spontaneously activated in mantle cell lymphoma (MCL) cell lines and patient's samples. *Eur J Cancer.* 2014;50(1): 159-169.
16. Pérez-Galán P, Roué G, Villamor N, Montserrat E, Campo E, Colomer D. The proteasome inhibitor bortezomib induces apoptosis in mantle-cell lymphoma through generation of ROS and Noxa activation independent of p53 status. *Blood.* 2006;107(1):257-264.
17. Weniger MA, Rizzatti EG, Pérez-Galán P, et al. Treatment-induced oxidative stress and cellular antioxidant capacity determine response to bortezomib in mantle cell lymphoma. *Clin Cancer Res.* 2011;17(15):5101-5112.
18. Witzig TE, Nowakowski GS, Habermann TM, et al. A comprehensive review of lenalidomide therapy for B-cell non-Hodgkin lymphoma. *Ann Oncol.* 2015;26(8):1667-1677.
19. Gribben JG, Fowler N, Morschhauser F. Mechanisms of Action of Lenalidomide in B-Cell Non-Hodgkin Lymphoma. *J Clin Oncol.* 2015; 33(25):2803-2811.
20. Wiestner A. Targeting B-Cell receptor signaling for anticancer therapy: the Bruton's tyrosine kinase inhibitor ibrutinib induces impressive responses in B-cell malignancies. *J Clin Oncol.* 2013;31(1):128-130.
21. Advani RH, Buggy JJ, Sharman JP, et al. Bruton tyrosine kinase inhibitor ibrutinib (PCI-32765) has significant activity in patients with relapsed/ refractory B-cell malignancies. *J Clin Oncol.* 2013; 31(1):88-94.
22. Wang ML, Rule S, Martin P, et al. Targeting BTK with ibrutinib in relapsed or refractory mantle-cell lymphoma. *N Engl J Med.* 2013;369(6):507-516.
23. Herishanu Y, Katz BZ, Lipsky A, Wiestner A. Biology of chronic lymphocytic leukemia in different microenvironments: clinical and therapeutic implications. *Hematol Oncol Clin North Am.* 2013;27(2):173-206.
24. Herishanu Y, Pérez-Galán P, Liu D, et al. The lymph node microenvironment promotes B-cell receptor signaling, NF-kappaB activation, and tumor proliferation in chronic lymphocytic leukemia. *Blood.* 2011;117(2):563-574.
25. Davis RE, Ngo VN, Lenz G, et al. Chronic active B-cell-receptor signalling in diffuse large B-cell lymphoma. *Nature.* 2010;463(7277):88-92.
26. Treon SP, Tripsas CK, Meid K, et al. Ibrutinib in previously treated Waldenström's macroglobulinemia. *N Engl J Med.* 2015;372(15): 1430-1440.
27. Treon SP, Xu L, Yang G, et al. MYD88 L265P somatic mutation in Waldenström's macroglobulinemia. *N Engl J Med.* 2012;367(9): 826-833.
28. Beà S, Valdés-Mas R, Navarro A, et al. Landscape of somatic mutations and clonal evolution in mantle cell lymphoma. *Proc Natl Acad Sci USA.* 2013;110(45):18250-18255.
29. Rosenwald A, Wright G, Wiestner A, et al. The proliferation gene expression signature is a quantitative integrator of oncogenic events that predicts survival in mantle cell lymphoma. *Cancer Cell.* 2003;3(2):185-197.
30. Ni T, Yang Y, Hafez D, et al. Distinct polyadenylation landscapes of diverse human tissues revealed by a modified PA-seq strategy. *BMC Genomics.* 2013;14:615.
31. Wang K, Singh D, Zeng Z, et al. MapSplice: accurate mapping of RNA-seq reads for splice junction discovery. *Nucleic Acids Res.* 2010; 38(18):e178.
32. Kaplan EL, Meier P. Nonparametric-estimation from incomplete observations. *J Am Stat Assoc.* 1958;53(282):457-481.
33. Klein JP, Moeschberger ML. Survival Analysis: Techniques for Censored and Truncated Data. 2nd ed. New York, NY: Springer; 2003.
34. Lam LT, Davis RE, Pierce J, et al. Small molecule inhibitors of IkappaB kinase are selectively toxic for subgroups of diffuse large B-cell lymphoma defined by gene expression profiling. *Clin Cancer Res.* 2005;11(1):28-40.
35. Ek S, Dictor M, Jerkeman M, Jirström K, Borrebaeck CA. Nuclear expression of the non B-cell lineage Sox11 transcription factor identifies mantle cell lymphoma. *Blood.* 2008;111(2): 800-805.
36. Kuo PY, Leshchenko VV, Fazzari MJ, et al. High-resolution chromatin immunoprecipitation (ChIP) sequencing reveals novel binding targets and prognostic role for SOX11 in mantle cell lymphoma. *Oncogene.* 2015;34(10):1231-1240.
37. Vegliante MC, Palomero J, Pérez-Galán P, et al. SOX11 regulates PAX5 expression and blocks terminal B-cell differentiation in aggressive mantle cell lymphoma. *Blood.* 2013;121(12):2175-2185.
38. Hildebrand JM, Luo Z, Manske MK, et al. A BAFF-R mutation associated with non-Hodgkin lymphoma alters TRAF recruitment and reveals new insights into BAFF-R signaling. *J Exp Med.* 2010;207(12):2569-2579.
39. Yang Y, Schmitz R, Mitala J, et al. Essential role of the linear ubiquitin chain assembly complex in lymphoma revealed by rare germline polymorphisms. *Cancer Discov.* 2014;4(4): 480-493.
40. Refaeli Y, Young RM, Turner BC, Duda J, Field KA, Bishop JM. The B cell antigen receptor and overexpression of MYC can cooperate in the genesis of B cell lymphomas. *PLoS Biol.* 2008; 6(6):e152.
41. Hermine O, Lefrère F, Bronowicki JP, et al. Regression of splenic lymphoma with villous lymphocytes after treatment of hepatitis C virus infection. *N Engl J Med.* 2002;347(2):89-94.
42. Iacovelli S, Hug E, Bennardo S, et al. Two types of BCR interactions are positively selected during leukemia development in the Eμ-TCL1 transgenic mouse model of CLL. *Blood.* 2015;125(10): 1578-1588.
43. Byrd JC, Furman RR, Coutre SE, et al. Targeting BTK with ibrutinib in relapsed chronic lymphocytic leukemia. *N Engl J Med.* 2013;369(1):32-42.
44. Wilson WH, Young RM, Schmitz R, et al. Targeting B cell receptor signaling with ibrutinib in diffuse large B cell lymphoma. *Nat Med.* 2015; 21(8):922-926.
45. Fontan L, Yang C, Kabaleeswaran V, et al. MALT1 small molecule inhibitors specifically suppress ABC-DLBCL in vitro and in vivo. *Cancer Cell.* 2012;22(6):812-824.

Downloaded from http://ashpublications.net/blood/article-pdf/128/1/82/1395848/82.pdf by guest on 02 June 2024